

EIGHTEENTH EUROPEAN ROTORCRAFT FORUM

1-05

Paper N° 138

A GENERIC TILT-ROTOR SIMULATION MODEL WITH PARALLEL  
IMPLEMENTATION AND PARTIAL PERIODIC TRIM ALGORITHM

J. S. G. McVicar

Research Student

R. Bradley

Senior Lecturer

University of Glasgow

September 15-18, 1992

AVIGNON, FRANCE

ASSOCIATION AERONAUTIQUE ET ASTRONAUTIQUE DE FRANCE



# A Generic Tilt-Rotor Simulation Model with Parallel Implementation and Partial Periodic Trim Algorithm

J. S. G. McVicar

and

R. Bradley

Department of Aerospace Engineering  
University of Glasgow  
Glasgow  
G12 8QQ  
Scotland

## Abstract

A generic tilt-rotor simulation model (GTILT) has been developed at the University of Glasgow. This model is centred round an individual blade rotor model which provides higher levels of fidelity than existing rotor disc models. However, individual blade models are numerically intensive and consequently most sequential programming facilities are unable to provide the performance necessary to make such models practical. In order to reduce computational run-times to an acceptable level GTILT has been parallelised and implemented on a computing surface. Another facet of individual blade models is that they generate periodic forces and moments when in the trim. Consequently, existing trimming algorithms formulated for use with quasi-steady disc models are inappropriate. A specialised partial periodic trimming algorithm has been developed and incorporated as part of GTILT; this algorithm is robust and has been found to produce rapid convergence. Longitudinal trim states predicted by GTILT have been verified against those of the Bell C81 model for a range of nacelle incidences and airspeeds with good correlation being obtained in all cases. GTILT has also been successfully employed to investigate the behaviour of the tilt-rotor configuration during transitional flight using a trim map to predict the control displacements necessary to produce a prescribed flight path during the transition phase.

## Nomenclature

$c$  Control state vector  
 $C_d$  Blade element drag co-efficient  
 $C_l$  Blade element lift co-efficient  
 $Ch$  Blade chord distribution  
 $J$  Jacobian matrix  
 $L$  Dynamic gains matrix  
 $L_a$  Rolling moment generated by rotor  
 $M_a$  Pitching moment generated by rotor  
 $M$  Apparent mass matrix  
 $n$  Number of blades per rotor

$p, q, r$  Fuselage roll, pitch and yaw rates about body axis set  
 $P_v$  Vehicle overall permutation matrix  
 $P_6$  Permutation matrix for a 3 bladed rotor with two flapping states per blade  
 $r_b$  Blade element spanwise location  
 $s$  Vehicle state vector  
 $s_l, s_r, s_{lf}, s_{fs}$  Left rotor, right rotor, induced flow and body axis flight state vectors  
 $T_a$  Thrust generated by rotor  
 $t_p$  Time for one period of oscillation in rotor forces and moments  
 $u_a, v_a, w_a$  Fuselage velocity components along x, y and z body axis respectively  
 $u_p, u_t$  Normal and tangential velocities at blade element  
 $w_{if}, p_{if}, q_{if}$  Uniform and harmonic rotor induced flow components  
 $V$  Magnitude of vehicle speed  
 $x_{fsCT}$  Current mean trim flight state vector  
 $x_{fsCFS}$  Current flight state vector  
 $x_{fsST}$  Specified mean trim flight state vector  
 $\alpha$  Blade element incidence  
 $\beta$  Blade flapping angle, fuselage sideslip angle  
 $\gamma$  Fuselage angle of climb  
 $\gamma_s, \dot{\gamma}_s, \ddot{\gamma}_s$  Shaft angle of tilt, angular velocity and acceleration  
 $\theta$  Fuselage pitch attitude  
 $\theta_{tw}$  Blade twist distribution  
 $\theta_{0c}, \theta_{0d}$  Combined and differential collective inputs  
 $\theta_{0l}, \theta_{0r}$  Collective blade pitch applied to left and right rotors  
 $\theta_{1sc}, \theta_{1sd}$  Combined and differential longitudinal cyclic inputs

$\theta_{1sl}, \theta_{1sr}$	Longitudinal cyclic applied to left and right rotors
$\theta_{1cc}$	Combined lateral cyclic input
$\theta_{1cl}, \theta_{1cr}$	Lateral cyclic applied to left and right rotors
$\Omega$	Fuselage turn rate
$\phi$	Fuselage bank attitude
$\psi_r$	Amount of rotor revolution from initial position.

## 1. Introduction

Tilt-rotor aircraft demonstrate significant potential by combining the VTOL capabilities of the helicopter with the long range, high speed performance of the conventional turbo-prop. As this potential is recognised proposals for future tilt-rotor aircraft vary greatly in terms of size and configuration, for example a recent research study, [1], suggests possible roles for five widely differing designs.

As these new configurations evolve it is important to have access to a generic simulation model at an early stage as this will enable the rapid evaluation of basic flight mechanic properties such as trim, performance and response over a wide range of flight conditions. In addition, a real-time capability provides scope for the development of control strategies for novel manoeuvres through an evaluation of the basic handling qualities. The aim of the current research has been two-fold, firstly, to develop a generic model capable of simulating a variety of tilt-rotor aircraft and, secondly, to investigate methods for its real-time operation.

Real-time performance has previously been achieved by using rotor disc models and rotor map models, [2,3]. These models sacrifice a degree of fidelity by assuming relatively simple blade aerodynamics and geometries. Modelling the behaviour of each rotor blade individually allows more complex blade aerodynamic and geometric characteristics to be specified and hence the accuracy is greatly improved. Additionally, the oscillatory behaviour of the rotor is now reflected because the rotor is not modelled as a whole but instead the contribution from each blade is considered individually. An individual blade model of this type has been developed at the University of Glasgow and is the subject of an earlier publication, [4]. Until recently few individual blade models, [5,6], have been used to support real-time simulations because their level of complexity has demanded prohibitive computational time.

When seeking an equilibrium, rotorcraft models driven by rotor disc/rotor map algorithms produce a constant flight state for a fixed set of control displacements. Zero rate of change of the state vector,  $[u_a, v_a, w_a, p, q, r, \theta, \phi]$ , is therefore experienced and this characteristic is generally used as

the criterion for defining when a trim state has occurred. A fixed control input to a model driven by an individual blade representation produces an equilibrium flight state which oscillates periodically about a fixed mean. The rates of change of the state variables will, therefore, only be zero when considered over a complete period which creates the requirement for a specialised trim algorithm.

It can therefore be seen that there is a requirement for a generic tilt-rotor model and that the fidelity would be greatly enhanced if the algorithm was driven by an individual blade model. Also it would be advantageous if the model could be used to support real-time simulation. However, the complexity of such a model creates difficulties when used for real-time simulation and produces the need for advanced computational hardware. Finally, the periodicity of the trimmed model generates the requirement for a specialised trimming method.

This paper describes a generic tilt-rotor model, (GTILT), which has been formulated round the individual blade model derived in a previous publication, [4]. Secondly it explains how the computational time has been greatly reduced by implementing the model on a transputer network of a suitable architecture. An algorithm designed to trim a rotorcraft model to a periodic flight state is derived and some predicted XV-15 trim states are compared with those of the Bell C81 model [3]. Finally, the results obtained from a transition study are presented.

## 2. The GTILT Model

The following main aspects have been included in the GTILT model:-

1. Two contra-rotating blade element rotor models.
2. Rotor induced velocity.
3. Rotor wake impingement on wing and horizontal stabiliser.
4. Aerodynamic characteristics of wing, fuselage and empennage.

and these will now be discussed in more detail.

### 2.1 Rotor Model

The rotor model incorporated in GTILT is as derived in Reference 4 and has been configured with XV-15 data which were obtained from Reference 3. In this model the blades are assumed to be identical, rigid and centre sprung providing a degree of freedom in flap. Each blade is divided into 10 equal spanwise elements for which there is the facility to use look-up tables describing the following parameters:-

$$C_l = f(\alpha, r_b, \text{Mach No})$$

$$C_d = f(\alpha, r_b, \text{Mach No})$$

$$\theta_{tw} = f(r_b)$$

$$Ch = f(r_b)$$

The spanwise variations of XV-15 blade twist and blade chord are as quoted in Reference 3. At present the lift co-efficient and drag co-efficient is defined as being constant along the whole span, this is due to the lack of available data and it is hoped to include more comprehensive parameters of the above form in the future.

Rotor control is provided by applying blade pitch deflections to the two side-by-side contra-rotating rotors, this yields the following five control states:-

1. Combined Collective.
2. Differential Collective.
3. Combined Longitudinal Cyclic.
4. Differential Longitudinal Cyclic.
5. Combined Lateral Cyclic.

An additional state, differential lateral cyclic, is possible but was considered to offer no practical benefit and was neglected.

In helicopter mode the above states provide control authority as given in table 2.1.

Axis	Control
Pitch	Combined Longitudinal Cyclic
Roll	Differential Collective + Combined Lateral Cyclic
Yaw	Differential Longitudinal Cyclic
Heave	Combined Collective

Table 2.1: GTILT Control States and their Authority in Helicopter Mode

The five control states are converted into blade pitch deflections according to the following expressions:-

$$\theta_{0l} = \frac{\theta_{0c} - \theta_{0d}}{2}, \quad \theta_{0r} = \frac{\theta_{0c} + \theta_{0d}}{2}$$

$$\theta_{1sl} = \frac{-\theta_{1sc} + \theta_{1sd}}{2}, \quad \theta_{1sr} = \frac{\theta_{1sc} + \theta_{1sd}}{2}$$

$$\theta_{1cl} = \frac{-\theta_{1cc}}{2}, \quad \theta_{1cr} = \frac{\theta_{1cc}}{2}$$

As can be seen a positive input of differential collective increases the collective of the right rotor relative to the left, thus, a positive displacement of this control will tend to generate a roll to the left.

Additionally, due to the fact that the rotors are rotating in opposite directions, an increase in collective of the right rotor relative to the left will generate an unbalanced reaction torque about the vehicle C.G. In this case a positive yawing moment is produced and the vehicle will tend to yaw to the right for a positive input of differential collective.

A positive input of combined longitudinal cyclic will incline both rotor surfaces aft, therefore, a positive displacement of this control will cause a pitch up of the vehicle. A positive input of differential longitudinal cyclic inclines the right rotor surface aft relative to the left and this will produce a yaw to the right.

A positive input of combined lateral cyclic inclines both rotors to the left and, thus, will generate a force and roll moment in that direction. Inputs to combined lateral cyclic and differential collective can be used in unison to control the vehicle bank attitude when in helicopter mode. This is the Lateral Translation Mode (LTM) and is described in Reference 6.

The rotor control states are washed out as a function of nacelle incidence with maximum authority being exerted in helicopter mode, the functions which wash these states out are as quoted in Reference 6.

## 2.2 Induced Velocity

The induced velocity model incorporated in GTILT is that of Peters and HaQuang [8]. This is a non-linear dynamic inflow model which describes the behaviour of three inflow states via a first order differential equation of the form given below in equation 2.2.1:-

$$[M] \begin{bmatrix} \dot{w}_{if} \\ \dot{p}_{if} \\ \dot{q}_{if} \end{bmatrix} + [L]^{-1} \begin{bmatrix} w_{if} \\ p_{if} \\ q_{if} \end{bmatrix} = \begin{bmatrix} T_a \\ L_a \\ M_a \end{bmatrix} \quad (2.2.1)$$

Where the apparent mass matrix,  $[M]$ , is a diagonal matrix which associates a lag with the response of the induced flow states following a control displacement or perturbation in flight state. The matrix  $[L]$  is the non-linear version of the dynamic gains matrix and relates the induced flow components to the aerodynamic rotor thrust, rolling and pitching moments. This matrix is non-diagonal in form and hence reflects a coupling between inflow states.

The rotor upwash on the horizontal stabiliser is modelled by incorporating wind tunnel data of Reference 9. Rotor wake impingement on the wing is included by superimposing the uniform induced flow component onto the freestream velocity with the

path of the downwash being assumed as parallel to the rotor shaft. No account is taken of the vehicle velocity when evaluating the path of the induced flow and therefore this component is assumed to travel parallel to the rotor shaft in all flight states. The area of the wing immersed in the wake is assumed equal to the circular arc directly below the rotor when the vehicle is flying in helicopter mode.

## 2.2 Vehicle Aerodynamics

The aerodynamic characteristics of the wing pylon and empennage are defined in "look-up" tables for  $C_l$  and  $C_d$  where the data were obtained from wind tunnel testing and are as quoted in Reference 3. The data for the wing pylon is quoted at four flap settings and two nacelle incidences, helicopter mode and aeroplane mode, with linear interpolation being employed for intermediate configurations. The tables are entered by angle of attack or sideslip angle; for the wing-pylon and horizontal stabiliser data are quoted in the range of  $\alpha$  between  $-90^\circ$  to  $+40^\circ$  and for the vertical surfaces in the range of  $\beta$  between  $-90^\circ$  and  $+90^\circ$ . Data for a range of empennage control displacements are also included with deflections of  $\delta_r$  and  $\delta_e$  in the range  $-20^\circ$  to  $+20^\circ$  being catered for. The modelling of the effect of aileron deflections is carried out by means of an aerodynamic effectiveness co-efficient.

The fuselage lift, drag, sideforce and pitching, yawing and rolling moment coefficients are obtained from a set of equations which approximate wind-tunnel data.

## 3 Parallelisation

As stated previously, the level of computational effort required by GTILT creates the necessity for an advanced computing system or supercomputer if run-times are to be maintained at an acceptable level. One method of reducing computational time is to structure the model as a set of sequential programs which can be run independently of each other and only interact to exchange information. These programs can be executed simultaneously on separate processors and, as the model has now been divided into concurrently running sections, major savings in run time are possible. GTILT has been parallelised in this way and implemented on a Meiko computing surface at The University of Glasgow; this will now be discussed.

The computing surface used contains 40 T800 transputers each of which is capable of loading and running its own piece of sequential code autonomously from the other processors on the surface. Four pairs of hard links are available to each transputer for the assembly of user defined topographies and, once connected, these links are used as communication paths between the transputers in

the network. Communication between computing surface and host terminal is achieved via the local host board which is connected to one transputer in the network through a pair of hard links. Soft links connect the network to various internal libraries which perform functions such as connecting transputers to the internal filing system, converting between message passing protocols or the routing of debugging messages to the user terminal.

The programming language native to the transputer is OCCAM and at the lowest level transputer topographies are formed using OCCAM harnesses. Code written in higher level languages can be compiled and linked to library files before being loaded onto the network by the configuring harness. However, in all but the simplest of cases problems arise when using this technique. Firstly, all the links necessary to form the topography must be specifically defined in the OCCAM harness and, secondly, when communicating between distant processes the information must be explicitly received and transmitted at each intermediate stage which leads to synchronization difficulties.

It is therefore preferable to generate transputer architectures and communicate between processes using a higher level method which does not require an OCCAM harness. This is made possible by the software package CS - Communicating Sequential - Tools which is run as a background process that makes the transputer architecture accessible to higher level languages. When using CS Tools, the required transputer architecture and distribution of processes on that domain is specified by means of an OCCAM PAR file. When executed at run time the CS Tools software forms all the necessary hard and soft links to produce the topography specified in the PAR file. Also, programs written in higher level languages can be compiled and linked to object files before being loaded onto the network, the distribution of these processes being specified in the PAR file.

Communication using CS Tools is carried out by means of a facility called the Computing Surface Network (CSN) which is a background OCCAM process that runs on all transputers in the network. The CSN is accessed by the FORTRAN code through a library of CS Tools functions which are used to transmit and receive information. When transmitting data the source need only specify its destination process and the underlying software performs all the necessary routing. This greatly simplifies inter-processor communication and enhances performance because it is no longer necessary to explicitly relay information at each intermediate stage. Also, the CSN selects the optimum route for the communication to follow so that if the most direct path is busy the next best alternative is selected.

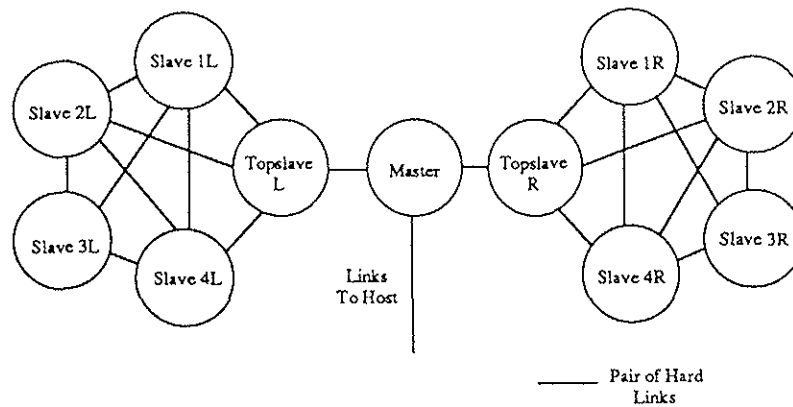


Figure 3.1: Transputer Topography Used in the Parallel Implementation of GTILT

### 3.1 Topography Used in the Parallelisation of GTILT

GTILT is formulated to be generic in nature therefore it is capable of modelling a range of vehicles irrespective of the number of rotor blades they have. When GTILT was parallelised it was designed to model the behaviour of each blade using code running on a dedicated transputer. To allow a reasonable degree of flexibility a single topography should be capable of supporting simulations for a range of vehicles each with a different number of rotor blades. Existing tilt-rotors and proposed future designs [1] all have three blades per rotor and few rotorcraft have more than five blades per rotor, hence, it was felt that a topography which could support simulations of vehicles with between one and five blades per rotor would provide adequate scope for future development. GTILT has been parallelised and implemented on the transputer topography shown in figure 3.1.

It can be seen that the topography reflects the physical geometry of the vehicle being modelled. The left and right groups of slaves are used to model the behaviour of the corresponding rotor with each slave representing an individual blade. The processor which links the two groups of slaves together is the master which models the vehicle aerodynamics and contains the solver for the equations of motion. All interactions with the user are carried out by the master, hence, it is run on processor zero which is most closely linked to the user terminal.

The communication paths have been established to minimise the distance between the processes which most frequently interact. The topslave controls all the slaves on its rotor and consequently it requires to communicate with them regularly, therefore, good communication links should exist between topslave and its slaves. Additionally, most communications between master and slaves must first be processed by the topslave (eg. the conversion of body axis cg velocities and accelerations to the corresponding parameters for the rotor hub in shaft axis), hence, the topslave also requires to be close to the master. It would be advantageous if the topslave could be

directly connected to all its slaves and the master, however, only four link pairs are available to each transputer so this level of networking is not possible. As a result the topslave is not directly connected to slave 3, consequently, for data to be transferred between these two processors it must first pass through one intermediate stage. It can be seen that slave 3 is most distant from the master and should only be used if five bladed rotors are to be modelled.

A large number of links exist between the slaves which form each 'rotor' and these links provide alternative communication paths should one route be busy. For example, if the topslave wished to communicate with slave 3 then CS Tools can transmit the data along three alternative routes all of which are the same length. Therefore, these additional paths prevent a delay in communication should one route be blocked.

### 3.2 Parallel Implementation of GTILT

The transputers are organised in an hierarchical order with each processor running a section of sequential FORTRAN code which models the behaviour of one component of the vehicle. The functions carried out by each process can be summarised as follows:-

1. The master process is responsible for:-
  - a) Performing all interactions with user.
  - b) Governing the actions of the topslave and slave processes.
  - c) Calculating the aerodynamic forces and moments acting on the vehicle.
  - d) Integrating the vehicle equations of motion.
2. The topslave process is responsible for:-
  - a) Governing the actions of the slaves under its control.
  - b) Calculating the flap, thrust, forces and moments of blade 1.

- c) Integrating the inflow states at each time step.
- d) Summing the individual blade components to calculate the overall rotor forces and moments in body axis.

3. The slave process is responsible for:-

- a) Calculating the flap, thrust, forces and moments of its blade.

The parallel scheduling of operations for one time step of a simulation for a vehicle with three blades per rotor is shown below in figure 3.2.

### 3.3 Synchronisation of Communications

When using the CS Tools software to communicate between processors the recipient process cannot selectively accept transmissions in a pre-determined order but instead receives in the order that the transmissions are made. As all individual processes run sequentially then the order of message transmission from each process is fixed, however, as the processes run concurrently then the sequencing of transmissions from different sources may vary. In order to prevent processes receiving communications out of phase with the sequence of appropriate recipient function calls some form of flagging is required. This method of message synchronisation is

exemplified by the interchange carried out between master and topslaves at the beginning of each time step. Here the master flags the topslaves to indicate that it has finished passing the body axis C.G. velocities and accelerations to the slaves. The topslaves are now free to transmit their shaft axis rotor hub velocities and accelerations to the slave processes. This exchange is necessary to prevent the communications to the slaves becoming out of phase with the corresponding recipient function calls, in which case the slaves would confuse the communication from the topslave as being the C. G. body axis velocity and accelerations transmission from the master. This kind of error is difficult to trace because the inclusion of debugging statements alters the execution speeds of the sequential processes and hence changes the phasing of message transmissions.

Flagging is best used when a series of communications which vary in size, or concern information widely differing in nature, is expected because this creates the need for a sequence of dedicated recipient function calls at the destination process. One drawback of this method occurs when a process runs slower than expected and is consequently late in transmitting which causes subsequent transmissions to block until the tardy communication is completed. When a process is receiving groups of similar data from separate sources, for example, when

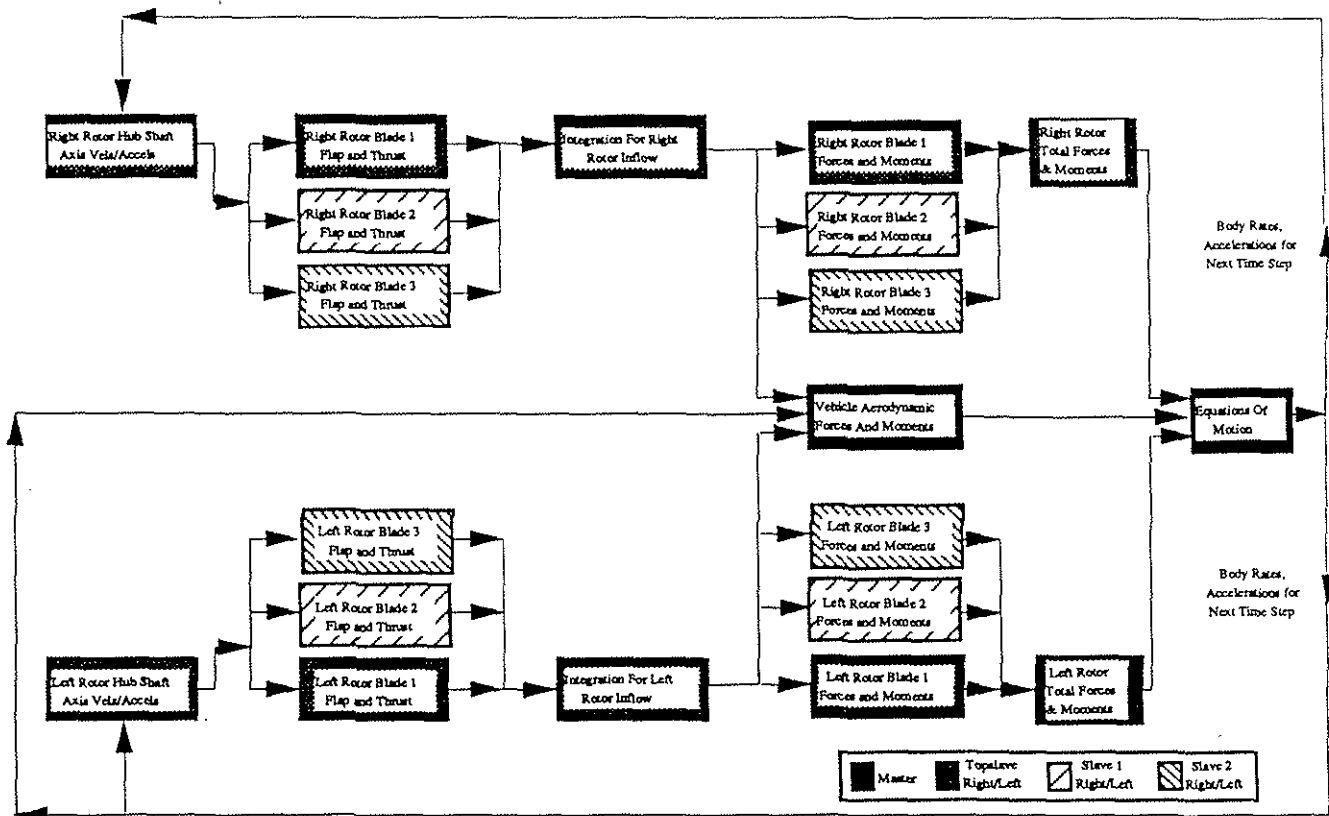


Figure 3.2: Scheduling of Processors in Parallelised Version of GTILT



the topslave receives the individual blade flap states from the slaves, then the time for communication can be reduced if the destination process receives the information using a 'generic' function call. Now data can be communicated in the order that the source processes are ready to transmit. When necessary, the communication's source can be marked by transmitting a one dimensional array of information, the first element of which contains an integer identifying the source process with subsequent elements containing the relevant information.

#### 4 Partial Periodic Trim Algorithm

The majority of existing rotorcraft algorithms incorporate quasi-steady disc models to describe the behaviour of the rotor [2,3]. For a fixed flight state this leads to the prediction of constant rotor forces and moments. Additionally, since the solution is carried out in multi-blade coordinates, the trimmed blade flap is described by non-time varying parameters. As none of the driving influences are oscillatory, a trim state can be said to have occurred when the vehicle adopts a constant flight state or, more directly, when the equations of motion yield zero rates of change in the flight states. Therefore, in order to obtain the required controls to produce a given trimmed flight state one sets the acceleration terms in the equations of motion to zero and performs an iteration in the control displacements until the flight state converges to the specified condition.

GTILT is driven by a more sophisticated rotor model [4] in which the equations are nonlinear and the trimmed solutions are periodic. As the equations of motion reflect any periodicity in the rotor forces and moments the vehicle will adopt a periodic rather than constant flight state when in the trim. Also, blade flapping behaviour is now modelled using individual blade coordinates, hence, trimmed blade flap is described by periodic parameters. This periodicity in trimmed flight state and trimmed blade flap leads to a relatively complex enigma when seeking the correct control input to produce a given trim state. Now one is faced with solving two interlinked problems simultaneously; one must ascertain the required control input to achieve the desired mean flight state whilst concurrently calculating the correct initial conditions to ensure periodicity in that flight state.

The trimming algorithm used in previous rotorcraft models which incorporate rotor disc representations is therefore inadequate and an alternative method is now required.

Given dynamic stability and a fixed control input, the most straightforward way to establish the corresponding trim state would be to integrate the equations of motion until the vehicle adopted a periodic flight state. This could be used as a basis for an iteration scheme to obtain the control input required to trim the vehicle to a given flight state,

however, this method faces two major problems. Firstly, the point at which the trim had been achieved would be unclear; ascertaining when the transients had decayed to zero and the remaining oscillations were purely due to the periodic trim could introduce errors which effect the performance of the iteration. Secondly, for each iteration a finite length of time would elapse before the flight state settled to its trim condition, thus, if the system were lightly damped, the computing time for convergence could be prohibitively long. In the worst case an initial guess near a stability boundary could produce divergent transients and the scheme would fail to converge. Hence it was concluded that this method was also unsuitable and that a more reliable alternative should be sought.

One method of obtaining the required controls and initial conditions to obtain a given trimmed periodic flight state is that of Periodic-Shooting/Newton-Raphson Iteration. An algorithm using this technique has been developed and incorporated into GTILT. The most appropriate starting point for the development of this algorithm is to clarify the definition of periodic trim with regard to rotorcraft simulation.

##### 4.1 Definition of Periodic Trim

The periodicity of the rotor model equations is a consequence of two factors influencing the behaviour of a rotor blade as it advances round the azimuth. Firstly, if a constant cyclic pitch is input then the blade angle of attack will vary periodically as it advances round the azimuth. Secondly if the vehicle has a constant non-zero velocity then the blade will experience a sinusoidal variation in the aerodynamic velocity as it rotates round the disc. Both these effects cause the rotating blade to generate periodic forces and moments in trimmed flight.

The period of oscillation for the trimmed rotor forces and moments is dependent upon the number of blades in the rotor. This is because each azimuthal position has its own associated blade pitch and aerodynamic velocity, thus for identical blades, each blade will generate the same contribution to the rotor forces and moments as it passes through that position. Thus, an  $n$  bladed rotor has to rotate through  $2\pi/n$  radians to have had, instantaneously, a blade in all azimuthal positions; therefore the full period of trimmed rotor forces and moments is described in  $2\pi/n$  radians of revolution. When seeking a trim state for a given set of controls one is interested in the effect the forces and moments have on the vehicle's flight state. It is most convenient to consider body axis states because then the parameters defining the vehicle's flight state are directly related to the forces and moments through the equations of motion. It follows that the period of oscillation for the vehicle's body axis flight states are the same as that of the driving rotor forces and moments, hence,

the period of oscillation for the vehicle flight states will be described in  $2\pi/n$  radians of rotor revolution. It can therefore be seen that the vehicle has achieved a trimmed flight state when equation (4.1.1) is satisfied.

$$\begin{bmatrix} u_a \\ v_a \\ w_a \\ p \\ q \\ r \\ \theta \\ \phi \end{bmatrix}_{\psi_r=0} = \begin{bmatrix} u_a \\ v_a \\ w_a \\ p \\ q \\ r \\ \theta \\ \phi \end{bmatrix}_{\psi_r=\frac{2\pi}{n}} \quad (4.1.1)$$

From equation 2.2.1 it can be seen that the induced flow generated by the rotor is closely related to the rotor thrust, pitching and rolling moments. Therefore, the periodicity of the induced flow states will also be described in  $2\pi/n$  radians of rotor revolution. If the rotor is in trim then the induced flow will satisfy equation 4.1.2 given below:-

$$\begin{bmatrix} w_{ifr} \\ p_{ifr} \\ q_{ifr} \\ w_{ifl} \\ p_{ifl} \\ q_{ifl} \end{bmatrix}_{\psi_r=0} = \begin{bmatrix} w_{ifr} \\ p_{ifr} \\ q_{ifr} \\ w_{ifl} \\ p_{ifl} \\ q_{ifl} \end{bmatrix}_{\psi_r=\frac{2\pi}{n}} \quad (4.1.2)$$

As the rotor must rotate through  $2\pi$  radians for each blade to have passed through all azimuthal locations then the full period of the trimmed blade states is described in one complete revolution of the rotor. The period of the blade states is therefore independent of the number of blades in the rotor. Thus, for an  $n$  bladed model including two flapping states per blade equation 4.1.3 will be satisfied if the rotor is in trim.

$$\begin{bmatrix} \beta_1 \\ \dot{\beta}_1 \\ \beta_2 \\ \dot{\beta}_2 \\ \vdots \\ \vdots \\ \beta_n \\ \dot{\beta}_n \end{bmatrix}_{\psi_r=0} = \begin{bmatrix} \beta_1 \\ \dot{\beta}_1 \\ \beta_2 \\ \dot{\beta}_2 \\ \vdots \\ \vdots \\ \beta_n \\ \dot{\beta}_n \end{bmatrix}_{\psi_r=2\pi} \quad (4.1.3)$$

It is desirable to minimise the number of computations required to ascertain periodicity because this will reduce the convergence time of the following iteration scheme. From equations 4.1.1, 4.1.2 and 4.1.3 it is evident that one revolution of the rotor is required to check for periodicity in the blade states whereas the rotor need only rotate through  $2\pi/n$  radians to check for periodicity in the induced flow states and vehicle flight state.

Since the surface described by a trimmed rotor is constant in form and fixed in orientation it is possible to ascertain blade periodicity in  $2\pi/n$  radians of revolution. In order to produce this constant surface all the blades must follow the same trajectory as they advance round the rotor disc and, as each blade starts rotating from a different azimuthal position, there is a phase shift of  $2\pi/n$  radians between the path of each blade. A set of initial trimmed blade states therefore provides a description of the blade trajectory at discrete points round the rotor disc. Thus for a rotor in trim, the states of an arbitrary blade  $m$ , at  $\psi_r=2\pi/n$  degrees will map onto the initial states of an identical blade  $m+1$  when  $\psi_r=0$ . This characteristic can be exploited to ascertain rotor trim in  $2\pi/n$  degrees of revolution and reduces the number of computations required at each iteration by a factor proportional to  $1/n$ . This forms the basis of the definition for the behaviour of a trimmed blade and equation 4.1.4 expresses this in vector form.

$$\begin{bmatrix} \beta_1 \\ \dot{\beta}_1 \\ \beta_2 \\ \dot{\beta}_2 \\ \vdots \\ \vdots \\ \beta_{n-1} \\ \dot{\beta}_{n-1} \\ \beta_n \\ \dot{\beta}_n \end{bmatrix}_{\psi_r=\frac{2\pi}{n}} = \begin{bmatrix} \beta_2 \\ \dot{\beta}_2 \\ \beta_3 \\ \dot{\beta}_3 \\ \vdots \\ \vdots \\ \beta_n \\ \dot{\beta}_n \\ \beta_1 \\ \dot{\beta}_1 \end{bmatrix}_{\psi_r=0} \quad (4.1.4)$$

In equation 4.1.4 the require mapping is obtained by shifting the order of elements in the state vector, it is more convenient if the states are mapped by the inclusion of a permutation matrix and this is shown overleaf in equation 4.1.5.

$$\begin{bmatrix} \beta_1 \\ \dot{\beta}_1 \\ \beta_2 \\ \dot{\beta}_2 \\ \vdots \\ \beta_{n-1} \\ \dot{\beta}_{n-1} \\ \beta_n \\ \dot{\beta}_n \end{bmatrix}_{\psi_T = \frac{2\pi}{n}} = \begin{bmatrix} 0 & 0 & 1 & 0 & 0 & 0 & \dots & 0 & 0 \\ 0 & 0 & 0 & 1 & 0 & 0 & \dots & 0 & 0 \\ 0 & 0 & 0 & 0 & 1 & 0 & \dots & 0 & 0 \\ 0 & 0 & 0 & 0 & 0 & 1 & \dots & 0 & 0 \\ \dots & \dots & \dots & \dots & \dots & \dots & \dots & \dots & \dots \\ \dots & \dots & \dots & \dots & \dots & \dots & \dots & \dots & \dots \\ 0 & 0 & 0 & 0 & 0 & 0 & \dots & 1 & 0 \\ 0 & 0 & 0 & 0 & 0 & 0 & \dots & 0 & 1 \\ 1 & 0 & 0 & 0 & 0 & 0 & \dots & 0 & 0 \\ 0 & 1 & 0 & 0 & 0 & 0 & \dots & 0 & 0 \end{bmatrix} \begin{bmatrix} \beta_1 \\ \dot{\beta}_1 \\ \beta_2 \\ \dot{\beta}_2 \\ \vdots \\ \beta_{n-1} \\ \dot{\beta}_{n-1} \\ \beta_n \\ \dot{\beta}_n \end{bmatrix}_{\psi_T=0} \quad (4.1.5)$$

As can be seen the permutation matrix is the identity matrix with the non-zero elements shifted to the right by an amount corresponding to the number of states per blade. The flexibility of this definition is reflected by the ease in which more states per blade can be added, for example, two lagging states could be included by simply shifting the non-zero permutation elements a further two locations to the right.

The expressions given in equations 4.1.1, 4.1.2 and 4.1.5 can be combined to define the overall vehicle trim. For a vehicle with two three bladed rotors, three inflow states per rotor and two flapping states per blade the overall definition of vehicle trim becomes:-

$$s(\psi_T=2\pi/n) = P_V s(\psi_T=0) \quad (4.1.6)$$

where:-

$$s = \begin{bmatrix} s_{rR} \\ s_{rL} \\ s_{if} \\ s_{fS} \end{bmatrix}$$

$$P_V = \begin{bmatrix} P_6 & 0 & 0 & 0 \\ 0 & P_6 & 0 & 0 \\ 0 & 0 & I_6 & 0 \\ 0 & 0 & 0 & I_8 \end{bmatrix}$$

and:-

$s_{rR}$  and  $s_{rL}$  are the blade state vectors for the right and left rotors respectively.

$s_{if}$ , and  $s_{fS}$  are the induced flow and flight state vectors respectively.

$P_6$  is a 6x6 permutation matrix of the form given in equation 4.1.5.

$I_m$  is the mxm identity matrix.

If the above mapping were to be carried out over  $2\pi$  radians of rotor revolution, eg for a single bladed rotor, then the permutation matrix would become the identity matrix and the definition becomes an extension of that quoted in Reference 9.

The definition of trim given in equation 4.1.6 could be used as part of an iteration scheme to establish the initial conditions which ensure a trimmed periodic flight state for a given control input. This would only be of great benefit if the control displacements necessary to produce a given trimmed flight state were known. This definition has therefore been incorporated into a more complex scheme which determines both the necessary controls and initial conditions to produce a specified trimmed flight state. The derivation of this scheme is now discussed.

#### 4.2 Specification and Convergence of Periodic Tilt-Rotor Trim

Helicopters have four control states available to the pilot and thus four flight states can be directly controlled. Generally, trim algorithms reflect this degree of authority by allowing four trajectory axis flight states to be specified explicitly; the required control inputs are then ascertained by an iterative process during which the body attitudes are also found. In helicopter mode, a tilt-rotor has five control states available to the pilot and, as discussed in section 2.1, the additional state is used to control bank angle, therefore bank angle can now be specified as part of a requested trim state.

Rotorcraft simulations which incorporate quasi-steady rotor map/disc models yield constant trimmed flight states, thus the trimming iteration can be said to have converged when the current control input

produces a flight state satisfying the specified condition. The closest periodic equivalent to the quasi-steady convergence criteria is to consider the required trim to have been achieved when the time averaged integrals of the specified states converge to yield the required values. Thus for an individually bladed tilt-rotor model in helicopter mode the trim convergence criterion is as given in equation 4.2.1.

$$x_{fsCT} = \frac{1}{t_p} \int_{t_{p0}}^{t_p} x_{fsCFS} dt = x_{fsST} \quad (4.2.1)$$

where:-

$$x_{fs} = \begin{bmatrix} V \\ \beta \\ \gamma \\ \Omega \\ \phi \end{bmatrix}$$

V=vehicle total velocity.  
 $\beta$ =fuselage sideslip angle.  
 $\gamma$ =fuselage angle of climb.  
 $\Omega$ =turn rate.  
 $\phi$ =fuselage angle of bank.  
 $t_p$ =time for rotor to rotate through  
 $2\pi/n$  radians

Subscripts CT, CFS and ST indicate current mean trim, current flight state and specified mean trim respectively.

As stated previously one must solve two problems simultaneously when determining the necessary control displacements to achieve a specified periodic trimmed flight condition. It can be seen that one must obtain the control displacements required to satisfy equation 4.2.1 whilst concurrently ascertaining the correct initial conditions to ensure periodic trim by satisfying equation 4.1.6. By performing a first order Taylor expansion of these expressions this problem can be rewritten in a form suitable for solution by Newton-Raphson iteration and is as given in equation 4.2.1.

$$\begin{bmatrix} s(0) \\ c \end{bmatrix}_{i+1} = \begin{bmatrix} s(0) \\ c \end{bmatrix}_i$$

$$\begin{bmatrix} J_{11}-P_v & J_{12} \\ J_{21} & J_{22} \end{bmatrix}^{-1} \begin{bmatrix} s(2\pi/n)-P_v s(0) \\ x_{fsCT}-x_{fsST} \end{bmatrix} \quad (4.2.2)$$

where:-

c is the control state vector.  
J is the Jacobian matrix.

The iteration described above can now be used to concurrently evaluate the necessary controls and initial conditions to produce a specified periodic trim state.

## 5 Discussion of Results Produced by GTILT

### 5.1 Convergence of Partial Periodic Trimmer

Flight path and control iteration histories for a 240 Knot level flight trim in aeroplane mode are depicted in figures 5.1 and 5.2 respectively. As can be seen convergence is achieved in six iterations with the solution being closely approximated after only three iterations despite the fact that a fairly poor initial guess was made. The robustness of the trimming methodology is highlighted by the iteration history for the climb angle,  $\gamma$ , where a large angle of climb (greater than  $40^\circ$ ) is produced at the first iteration. Such a climb angle produces vehicle angles of attack outwith the range of the component look-up tables where the co-efficients have been assumed constant. Despite this, the iteration continues rapidly to convergence thus demonstrating the reliability of the trimming algorithm.

Similar iteration histories for a 10 Knot forward flight case with  $4^\circ$  bank angle in helicopter mode are given in figures 5.3 and 5.4. Again it can be seen that convergence is rapid with the required trimmed flight state being obtained in 4 iterations. With reference to figure 5.4 it is evident that displacements in all 5 controls are required to produce this trim. The input of combined collective generates the necessary thrust to balance the aerodynamic and gravitational forces acting on the vehicle with the longitudinal stick displacement being required to balance the pitching moment acting on the vehicle CG at the trimmed incidence and speed. The input of combined lateral cyclic, in this case about  $4^\circ$  per rotor, orientates the rotor thrust vectors to the vertical whilst the vehicle flies with  $4^\circ$  degrees angle of bank. This control displacement also generates an unwanted rolling moment which would tend to produce a roll to the left, hence, the input of lateral stick is required to offset this. In helicopter mode, the lateral stick displacement generates a rolling moment by increasing the collective of one rotor relative to the other, this also produces a yawing moment which, in this case, would tend to yaw the vehicle to the left. In order to balance the unwanted yawing moment an input of right pedal is required and the zero sideslip flight path maintained. The combination of controls described above is qualitatively valid as it forms a recognised strategy for maintaining a prescribed bank angle and is described in reference 7 as the Lateral Translation Mode.

## 5.2 Verification of GTILT

Adequate verification of GTILT has proved problematical due to the lack of available flight test data. However, it has been possible to compare predicted longitudinal XV-15 trim states with those of the Bell C-81 model using data published in Reference 3. Two examples of this exercise will now be discussed.

Figure 5.5 shows a comparison of the predicted longitudinal trim states for the vehicle in helicopter mode across a range of forward flight speeds.

With reference to this figure it can be seen that the predicted blade root pitch shows good agreement for trim speeds up to 40 Knots. Between 40 Knots and 80 Knots GTILT estimates that progressively more collective is required to produce the trim than does the Bell C81 with a maximum difference of 1.5 degrees occurring at 80 Knots. At trim speeds above 80 Knots correlation between the models improves with GTILT estimating the requirement of 0.5 degrees more collective to produce 140 knots trimmed flight. It is most probable that the disparities in predicted blade pitch are attributable to the modelling of the rotor wake impingement on the wing. For all flight speeds and configurations, GTILT assumes that the area of wing immersed in the wake is equal to the circular arc directly below the rotor when the vehicle is in helicopter mode. This approximation is valid when the velocity of the vehicle is negligible relative to the velocity of the induced flow, however, at higher flight speeds the rotor wake will be washed backwards and will impinge on a smaller wing area. This leads to a decreased induced download and consequently the amount of combined collective required to produce the trim is over predicted by GTILT. At high forward speeds the velocity of the rotor wake decreases to such an extent that the induced downforce is negligible and the approximation made in GTILT becomes less significant and correlation improves.

The longitudinal stick displacements required to produce trimmed flight show good agreement throughout the quoted speed range. Both models exhibit the same general trend of increasing forward longitudinal stick with trimmed airspeed and show a stick reversal occurring at the lower end of the quoted speed range. This reversal is generated as a result of the rotor upwash striking the horizontal stabiliser which has the net effect of generating a pitch down moment that has to be offset by a more aft input of longitudinal stick. At higher airspeeds the wing downwash on the horizontal stabiliser becomes more effective providing a stable stick gradient with increasing airspeed. In GTILT the modelling of the rotor wake is such that impingement on the horizontal stabiliser occurs when the vehicle is flying at a higher speed than in the Bell C81, consequently the stick reversal occurs at higher airspeed in GTILT.

In both models the vehicle pitch attitude becomes increasingly nose down as the trimmed forward speed increases, however, a small disparity exists between the models across the speed range. It is suspected that this is due to minor differences in the evaluation of the overall pitching moment which forces the vehicle to adopt a slightly different pitch attitude in order to achieve a moment balance.

Figure 5.6 shows a comparison of the predicted longitudinal trim states for the vehicle in aeroplane mode across a range of flight speeds.

It can be seen that good correlation exists between the two models for the predicted blade root pitch across the quoted range of trim speeds. However, the relationship between trim speed and required blade pitch is predicted as being non-linear by GTILT whereas the Bell model shows this as being linear. It is suspected that the difference is attributable to the evaluation of the rotor thrust. GTILT includes the normal component of velocity,  $u_p$ , when calculating the blade element dynamic pressure, consequently, rotor thrust is a function of  $(u_p + u_d)^2$ . This is reflected in the collective input required to produce trimmed flight by a non-linear variation with increasing  $u_p$ . The C81 model applies a linear correction factor onto the rotor thrust to include the effect of increasing  $u_p$  and this is reflected by the linear relationship between collective input and trimmed airspeed.

It is of interest to note that a larger input of collective is required to produce 140 knot trimmed flight in aeroplane mode than helicopter mode despite the fact that the rotors are producing considerably more thrust in the latter case. This is mainly because the significantly higher normal velocity component in aeroplane mode generates a reduction in the blade angle of attack which has to be offset by a larger collective input.

Excellent agreement is obtained for the predicted longitudinal stick displacement and vehicle pitch attitude required to produce trimmed flight. The difference in longitudinal stick displacement does not exceed 1% and the pitch attitude is predicted to within 1 degree throughout the quoted range.

## 5.3 Transitional Time Histories

Tilt-rotor aircraft exhibit highly non-linear behaviour throughout their flight envelope, mainly due to non-linear aerodynamic characteristics and strong coupling between control states, and this creates difficulties when attempting to force the vehicle to follow a prescribed flight path. One concept recognised to be of value when controlling the trajectory of vehicles with such non-linearities is the use of systems which incorporate model inversion in the feed forward path [11]. In this technique a fully

non-linear simulation model of the vehicle is continually inverted in real time to determine the control inputs necessary to produce the demanded flight path. A methodology similar to this has been used to predict the control inputs necessary to obtain a specified flight path during full transitions to and from aeroplane mode.

Essentially, the trimming algorithm described in section 4 performs a model inversion whereby a desired trajectory axis trim state is specified and the required controls ascertained. If a manoeuvre is divided into discrete intervals, then the trimming algorithm can be used to ascertain the necessary controls to recreate that manoeuvre at discrete points through its history. By linking this series of control inputs together a trim map which details the necessary scheduling of controls throughout the manoeuvre can be generated and subsequently used to drive the vehicle along the required flight path. This technique has been used to generate trim maps which predict the control inputs required for GTILT to follow a prescribed flight path during full transitions to and from aeroplane mode; these are given in figures 5.7 and 5.9 respectively.

When generating these trim maps the transition was broken down into six equal segments with the trim algorithm establishing the control inputs necessary to produce the specified flight path at the end of each interval. For a transition from helicopter to aeroplane mode the flight path was defined as follows:-

1. The transition is initiated 5 seconds into the simulation and completed 15 seconds later.
2. Initial velocity of 80 Knots with a linear acceleration to 120 Knots through the transition.
3. Zero angle of climb, turn rate, bank angle or sideslip throughout the manoeuvre.
4. A fifth order polynomial,  $\gamma_s(t)$ , was used to define the transitional profile of the nacelles with the coefficients being evaluated to satisfy suitable boundary conditions for  $\gamma_s$ ,  $\dot{\gamma}_s$  and  $\ddot{\gamma}_s$ .
5. Rotor speed and flap setting were maintained constant throughout the transition.

When transitioning from aeroplane to helicopter mode the above velocity and nacelle tilt profiles were reversed.

With reference to figures 5.7 and 5.9 it can be seen that the profile of longitudinal stick displacements required to produce this flight path is highly non-linear. This is attributable to the rotor wake and wing downwash modelling which causes the horizontal stabiliser to produce non-linear pitching moment variations with airspeed and nacelle incidence.

Flight path time histories for the transition from helicopter to aeroplane mode are given in figure 5.8. From this figure it can be seen that the requested linear acceleration from 80 Knots to 120 Knots is achieved with only a small, heavily damped oscillation being present at the end of the transition. The specified zero angle of climb is not achieved however and a maximum climb angle of  $-15^\circ$  is produced. It is suspected that this is because the trim map details the control inputs required to produce a series of steady state trims and consequently neglects the transitory vehicle dynamics generated when these states are linked together to form a flight path. The vehicle pitch attitude is unspecified when the trim map is constructed but can be seen to follow the sequence of longitudinal stick displacements.

Figure 5.8 also shows the accuracy by which the trim algorithm predicts the control displacements necessary to produce a specified trim. It can be seen that the specified trimmed aeroplane mode flight path is maintained for the duration of the simulation once the transition is completed.

With reference to figure 5.10 it can be seen that the specified flight path is poorly replicated when transitioning from aeroplane to helicopter mode. It is suspected that the phugoid mode is excited by the sequence on longitudinal stick displacements and this produces the oscillations in velocity, climb angle and pitch attitude. In helicopter mode the phugoid is lightly damped and consequently the steady state trim is not obtained until approximately 140 seconds after the transition is completed.

From figure 5.12 it can be seen that trim maps are more accurate when predicting the control displacements necessary to perform transitions carried out over a longer time period. In this case the transition is again to helicopter mode but is now carried out over 100 seconds and it is evident that the specified flight path is more closely replicated than in the 15 second transition. This is because the longitudinal stick displacements are input at a lower frequency and therefore do not excite the phugoid mode. Also, the vehicle accelerations are considerably reduced and consequently the manoeuvre more closely resembles the series of linked trim states on which the trim map was based.

## 6. Conclusions

1) A mathematical model, GTILT, which describes the behaviour of a generic tilt-rotor aircraft has been derived at the University of Glasgow; the main features of GTILT can be summarised as follows:-

- a) The rotor forces and moments are generated by two contra-rotating rotors each modelled by the individual blade algorithm derived in reference 4. This has provided high levels of fidelity by

allowing the inclusion of representative blade geometries and aerodynamic characteristics.

b) "Look-up" tables are included for the vehicle aerodynamic coefficients.

c) Rotor wake impingement on the wing and horizontal stabiliser is included. This has been found to have a significant effect on the overall vehicle pitching moment and therefore strongly influences the longitudinal stick positions required to produce trimmed flight or to perform a specified manoeuvre.

d) Control authority is exerted by both blade root pitch control and aerodynamic control surface deflections. The rotor control states are progressively washed out as the nacelles are tilted towards aeroplane mode with constant gains being incorporated throughout the flight envelope for the aerodynamic surface displacements.

2) Individual blade rotor models of the form used in GTILT are numerically intensive and consequently impractical when implemented on most sequential computing facilities. Computational run times have been reduced by parallelising GTILT which has enabled the model to be run concurrently on a computing surface.

3) Modelling the behaviour of each rotor blade individually produces periodicity in the rotor forces and moments, consequently, the trimmed flight path will also be periodic in nature. A specialised trimming algorithm has therefore been developed to ascertain the correct initial conditions and control states necessary to produce a given specified periodic trim state. This trim algorithm has been found to be robust and capable of producing rapid convergence for most specified trim states.

4) GTILT has been configured using XV-15 data from reference 3 and a series of predicted longitudinal trim states verified against those of the Bell C81 model. Generally correlation between the two models is excellent with the slight disparities present being mainly attributable to differences in the modelling of the rotor wake impingement on the wing and horizontal stabiliser.

5) The trim algorithm has been used to generate trim maps which predict the series of control displacements necessary to force the vehicle to follow a specified flight path during the transition phase. When transitioning from helicopter mode the trim map closely predicts the control displacements necessary to force the vehicle to follow a prescribed flight path during a 15 second transition. However, when transitioning from aeroplane mode the manoeuvre must be carried out over a longer time period in order to avoid the excitation of the vehicle phugoid mode.

## Acknowledgements

The authors wish to thank Dr Gareth Padfield of the Defence Research Agency, Bedford for his help and assistance during the development of the GTILT model.

## References

1. Bell-Boeing Study Team, "Civil Tilt-Rotor Missions and Applications: A Research Study", Summary Final Report NASA CR 177452, July 1987
2. Padfield, G. D., "A Theoretical Model of Helicopter Flight Mechanics for Application to Piloted Simulation", RAE TR81048, April 1981
3. Harendra, P. B. et al, "A Mathematical Model For Real Time Flight Simulation of the Bell Model 301 Tilt Rotor Research Aircraft", Bell Helicopter Company Report No. 301-099-001, April 1973
4. McVicar, J. S. G., Bradley, R., "A Generic Rotor Algorithm for Application to Real-Time Tilt-Rotor Simulation", University of Glasgow, Department of Aerospace Engineering Report No. 9015, September 1990
5. Du Val, R. W., "A Real-Time Blade Element Helicopter Simulation for Handling Qualities Analysis", Proceedings of the Fifteenth European Rotorcraft Forum, Amsterdam, September 1989
6. Meerwijk, L., Brouwer W., "Real-Time Helicopter Simulation Using the Blade Element Method", Proceedings of the Seventeenth European Rotorcraft Forum, Berlin, 1991
7. Bell-Boeing, "Tilt-Rotor Handling Qualities Short Course Notes"
8. Peters, D.A., HaQuang, N., "Dynamic Inflow for Practical Applications", Journal of the American Helicopter Society, Technical Note, October 1988
9. Marr, R. L., et al "V/STOL Tilt-Rotor Study. Volume 6. Hover, Low Speed and Conversion Tests of a Tilt-Rotor Aeroelastic Model (Model 300)", NASA CR 114615, May 1973
10. Peters, D. A., Izadpanah, A. P., "Helicopter Trim By Periodic Shooting with Newton-Raphson Iteration"
11. Smith, G. A., Meyer, G., "Aircraft Automatic Flight Control System with Model Inversion", Journal of Guidance and Control, Vol 10, No. 3, 1987

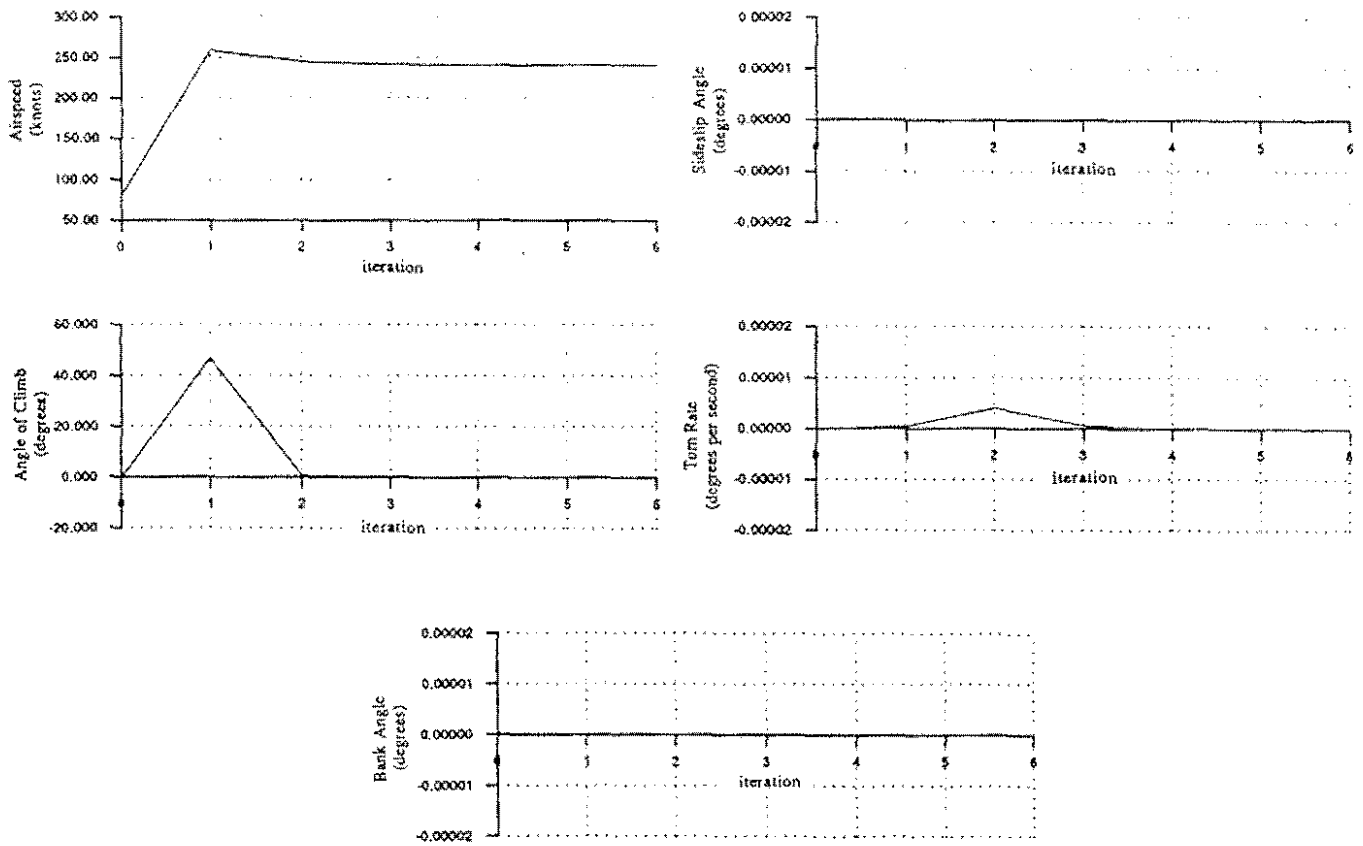


Figure 5.1: Flight Path Iteration History for 240 Knot Trimmed Level Flight in Aeroplane Mode

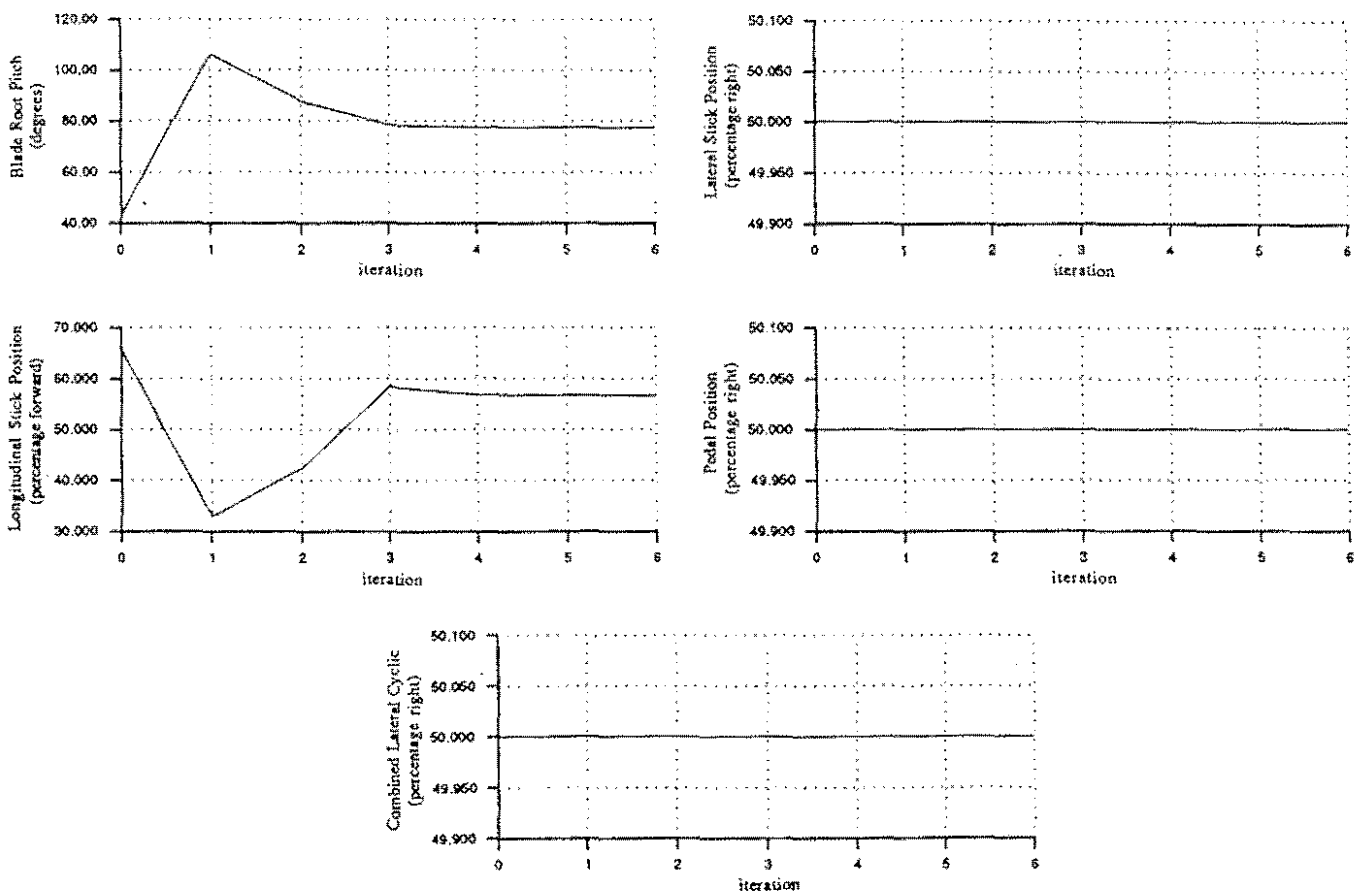


Figure 5.2: Control State Iteration History for 240 Knot Trimmed Level Flight in Aeroplane Mode



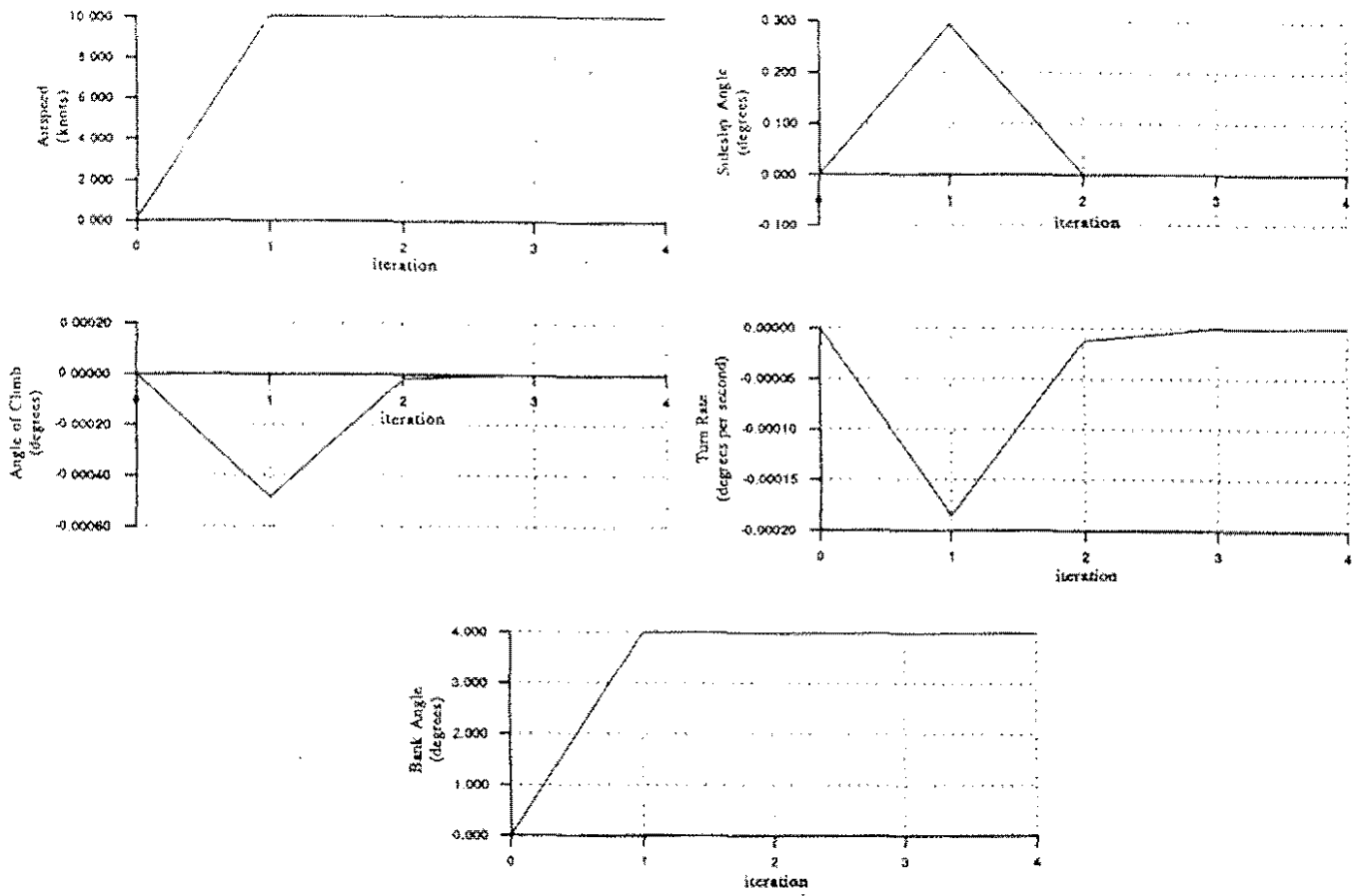


Figure 5.3: Flight Path Iteration History for 10 Knot Trimmed Flight with 4 Degrees of Bank in Helicopter Mode

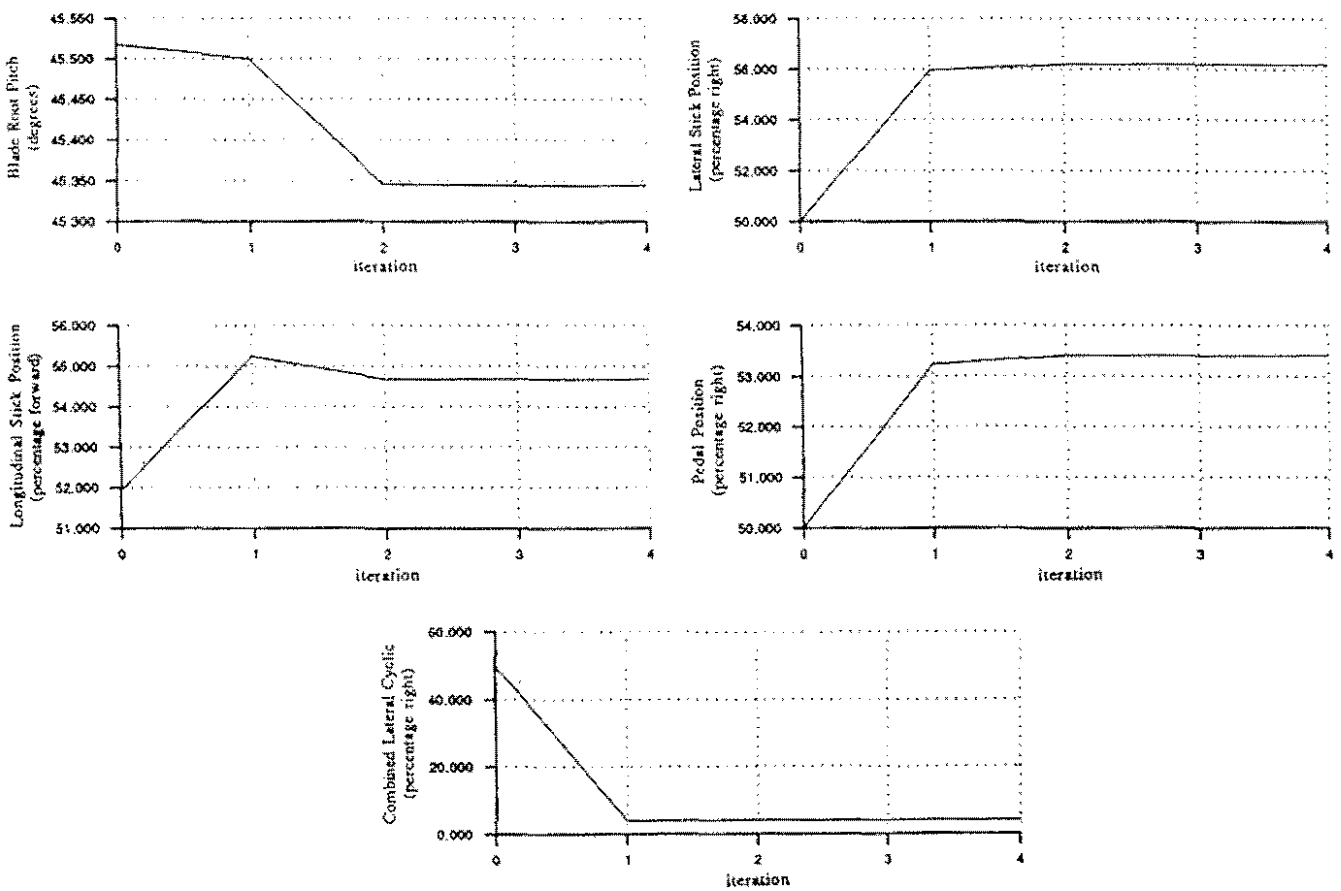


Figure 5.4: Control State Iteration History for 10 Knot Trimmed Flight with 4 Degrees of Bank in Helicopter Mode

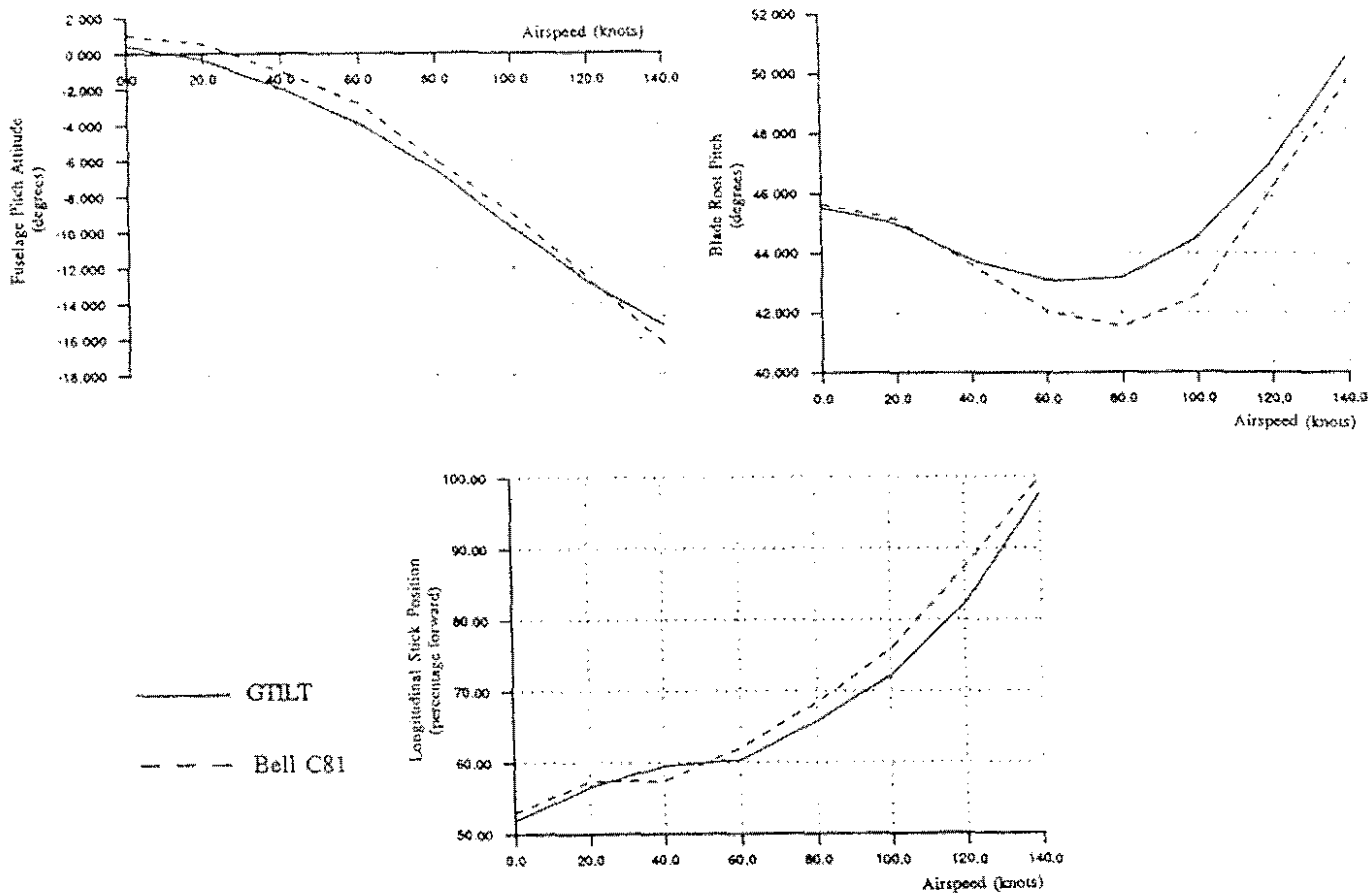


Figure 5.5: Comparison Between GTILT and Bell C81 Helicopter Mode Longitudinal Trim States

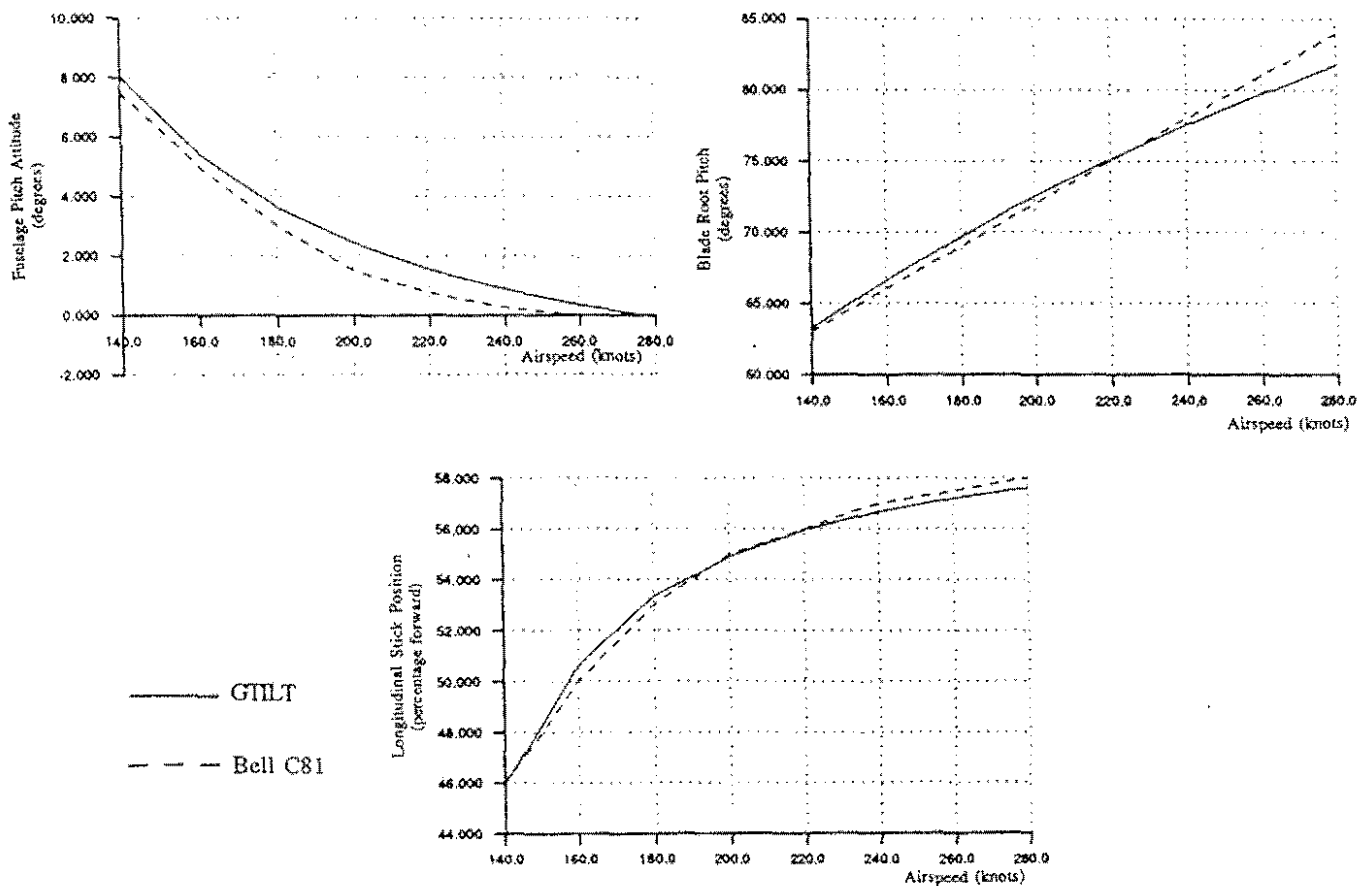


Figure 5.6: Comparison Between GTILT and Bell C81 Aeroplane Mode Longitudinal Trim States

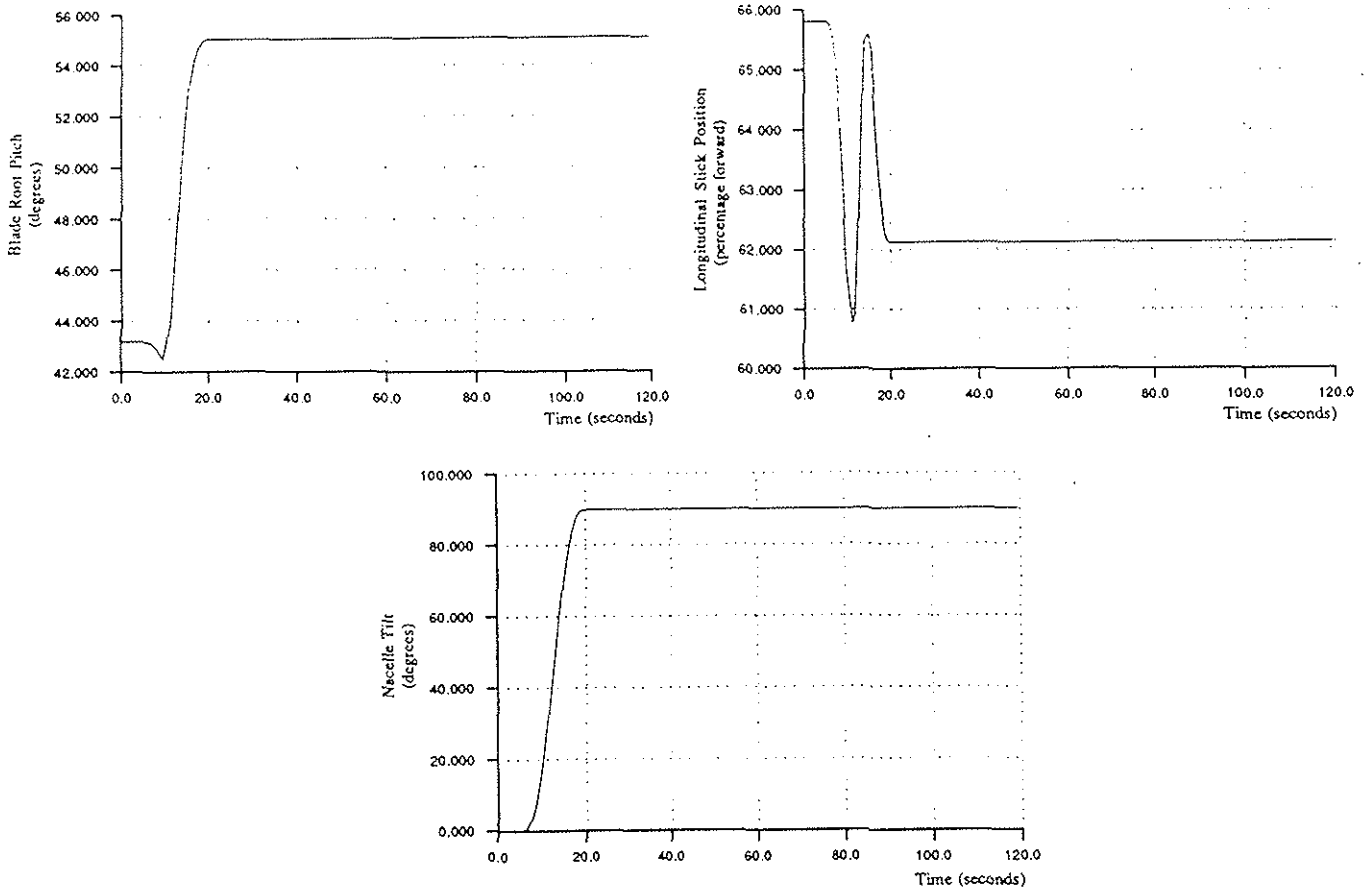


Figure 5.7: Predicted Trim Map of Control Displacements Necessary to Produce a 15 Second Level Flight Transition from Helicopter to Aeroplane Mode

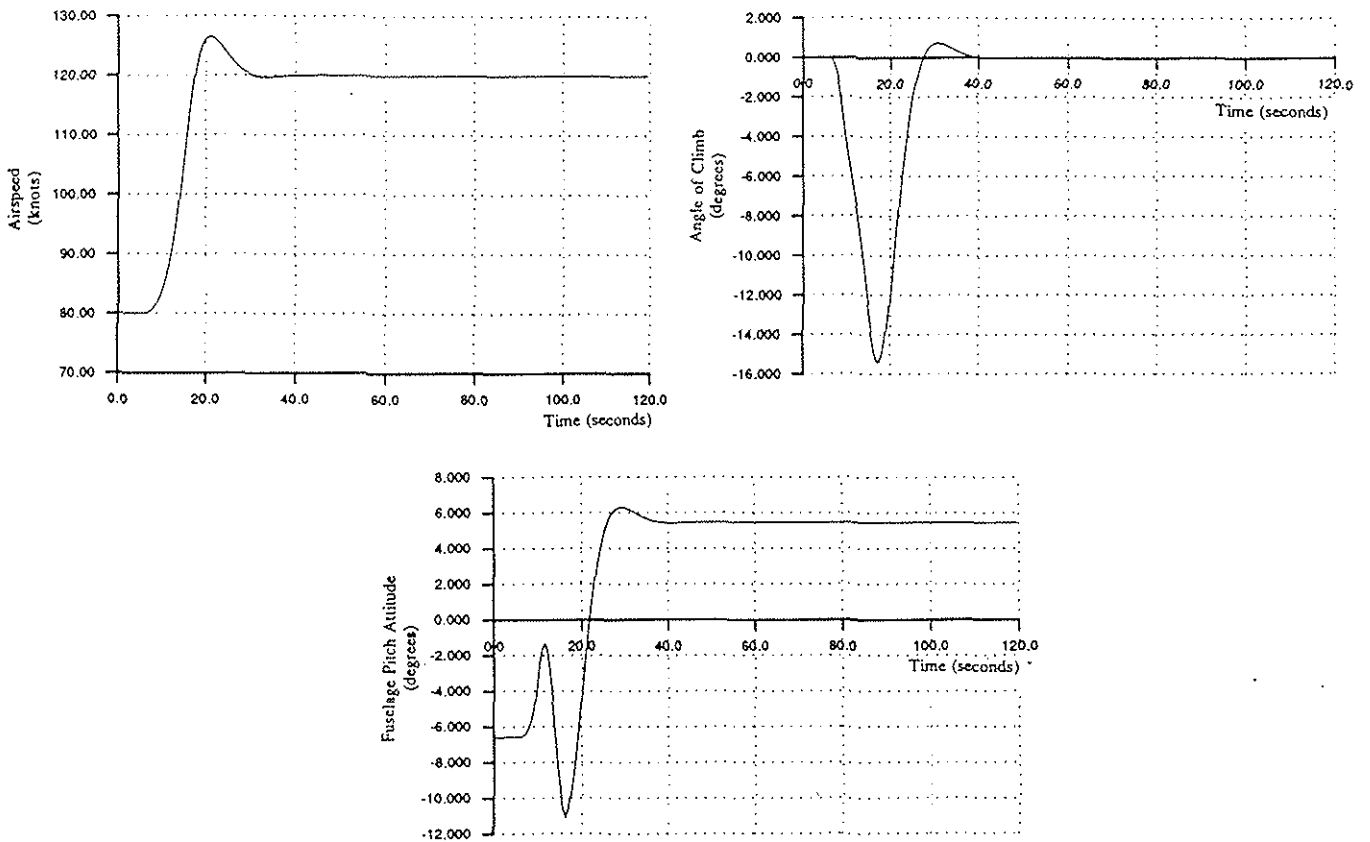


Figure 5.8: Flight Path Produced when Performing a 15 Second Transition from Helicopter to Aeroplane Mode Using Control Displacements as Described by a Trim Map

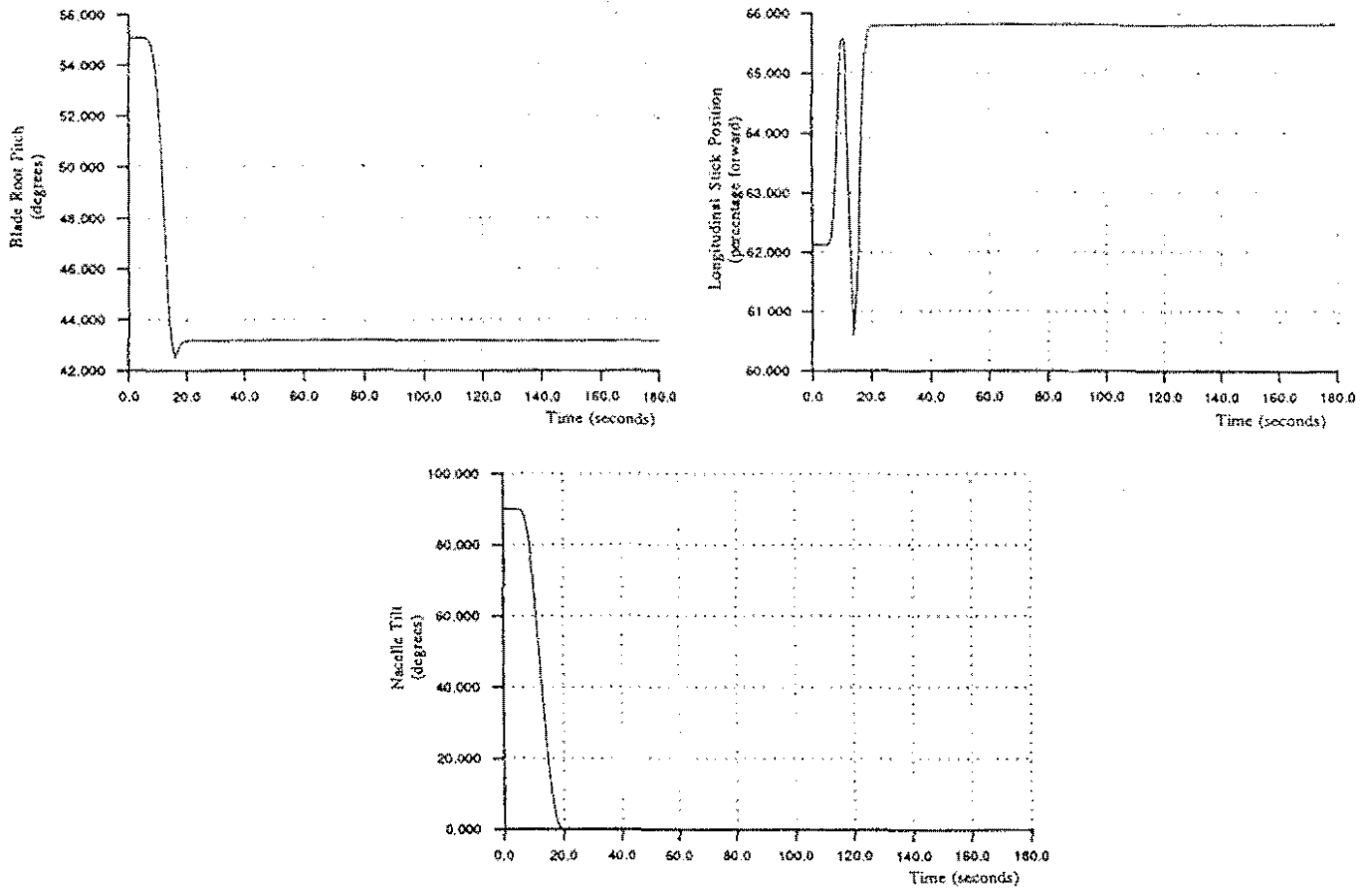


Figure 5.9: Predicted Trim Map of Control Displacements Necessary to Produce a 15 Second Level Flight Transition from Aeroplane to Helicopter Mode

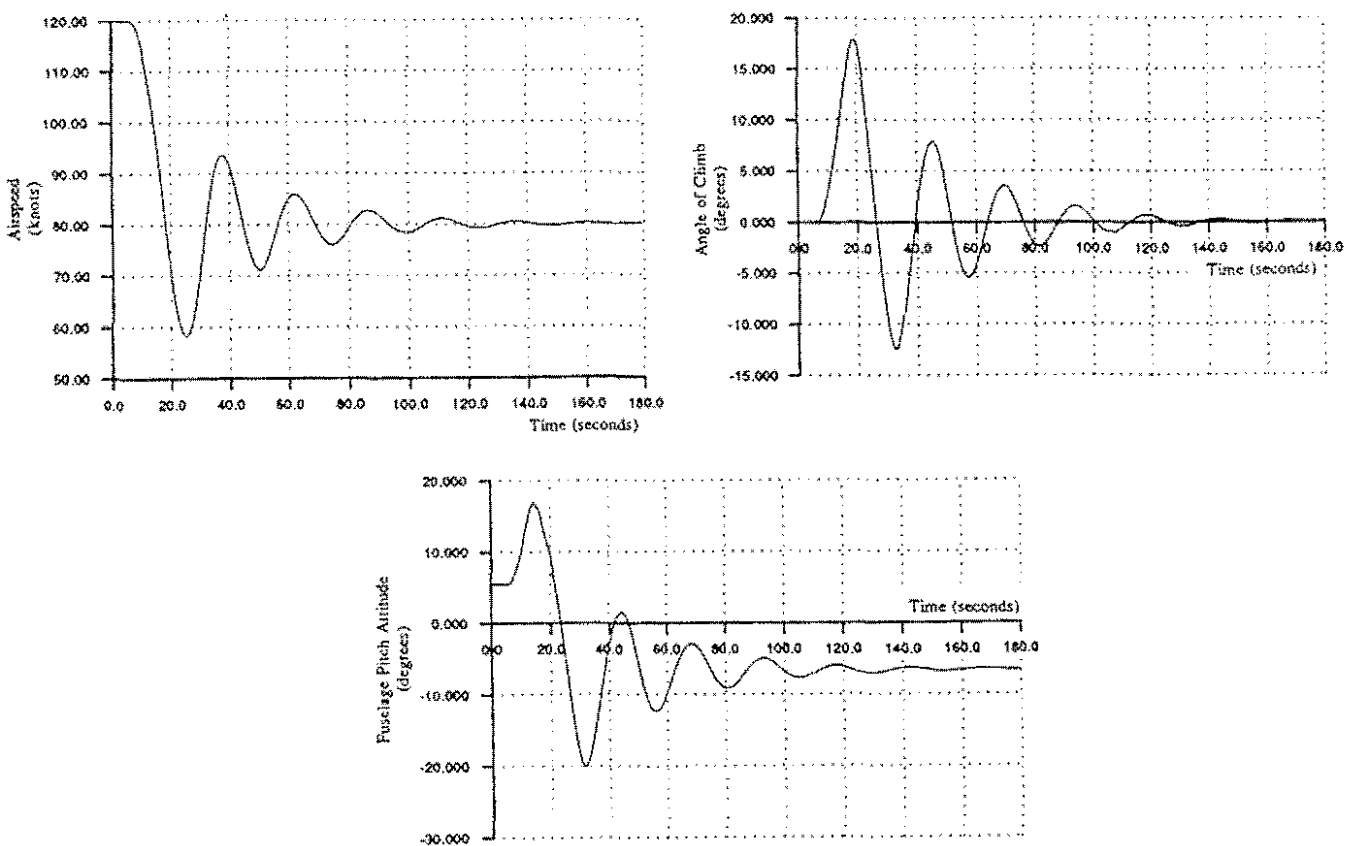


Figure 5.10: Flight Path Produced When Performing a 15 Second Transition from Aeroplane to Helicopter Mode Using Control Displacements as Described by a Trim Map

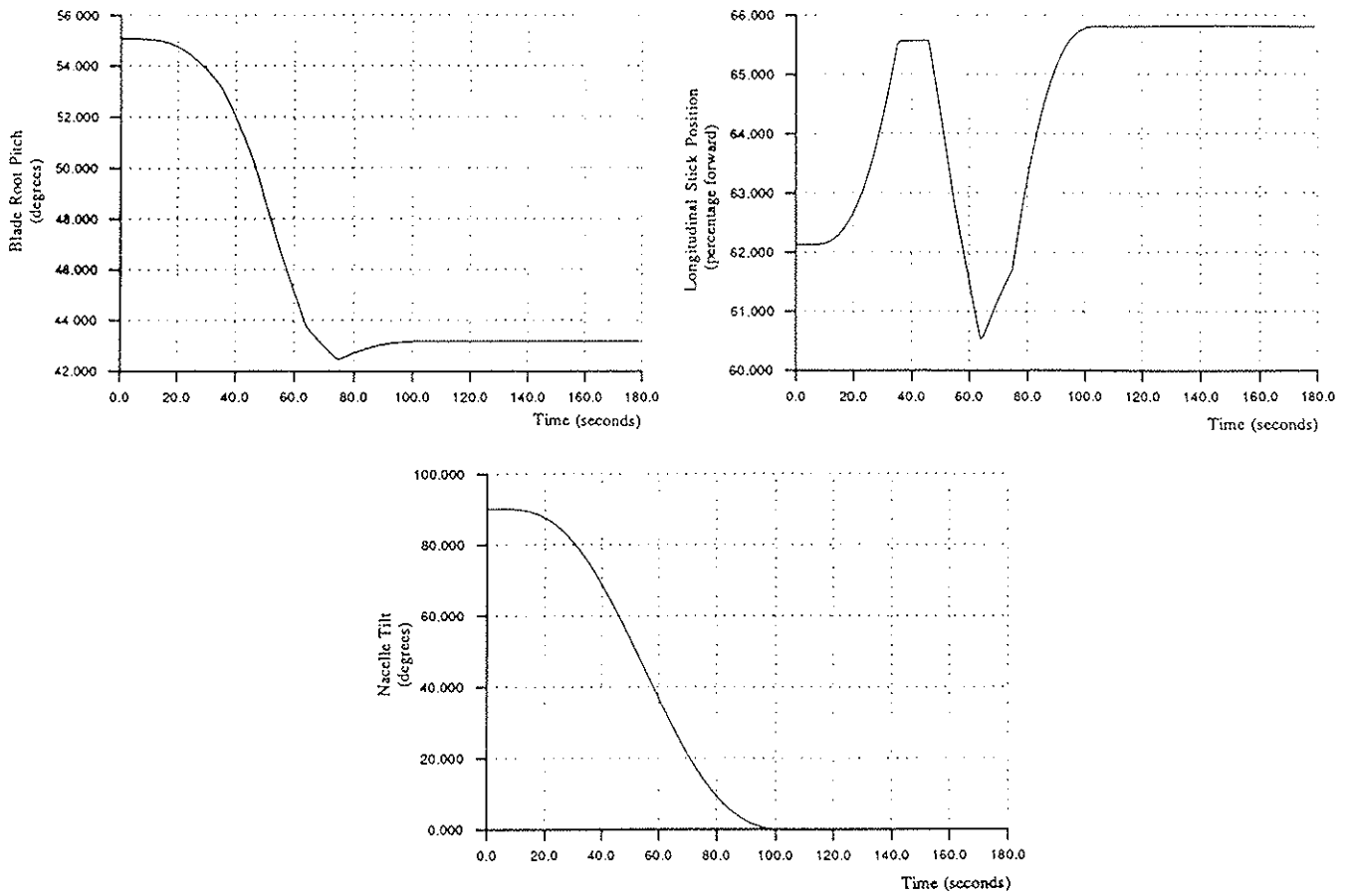


Figure 5.11: Predicted Trim Map of Control Displacements Necessary to Produce a 100 Second Level Flight Transition from Aeroplane to Helicopter Mode

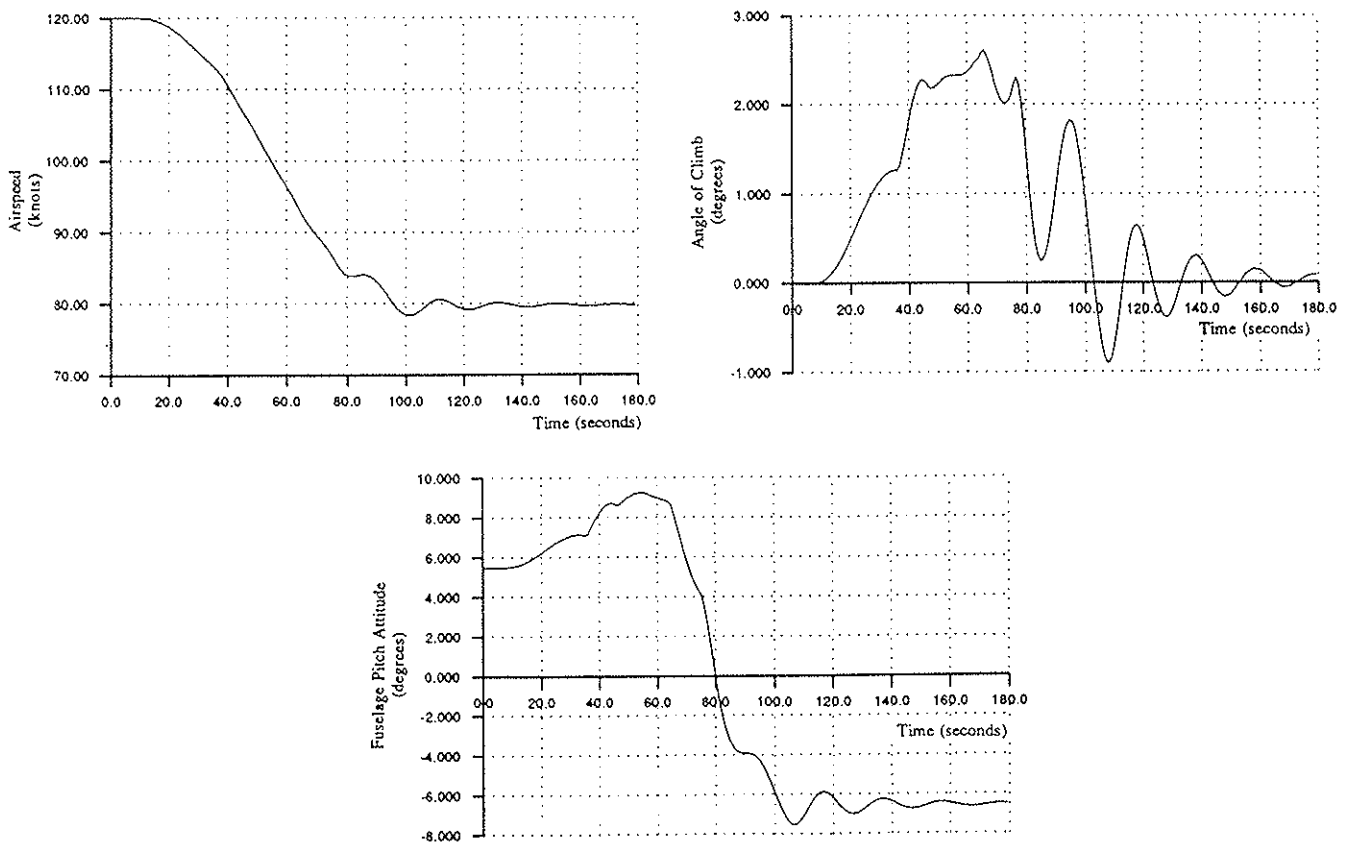


Figure 5.12: Flight Path Produced when Performing a 100 Second Transition from Aeroplane to Helicopter Mode Using Control Displacements as Described by a Trim Map